Supramolecular Chemistry
Publication details, including instructions for authors and subscription information:
http://www.informaworld.com/smpp/title~content=t713649759

Catalysis of Helix Inversion of Zinc Bilindiones by Amines and Amino Acid Esters

Tadashi Mizutani[a]; Shigeyuki Yagi[a]; Atsushi Honmaru[a]; Thorsten Goldacker[a]; Susumu Kitagawa[a]; Masaru Furusyo[b]; Toru Takagishi[c]; Hisanobu Ogoshi[d]
[a] Department of Synthetic Chemistry and Biological Chemistry, Graduate School of Engineering, Kyoto University, Kyoto, Japan [b] CAE Research Center, Sumitomo Electric, Ltd., Kyoto, Japan [c] Department of Applied Materials Science, Osaka Prefecture University, Sakai, Osaka, Japan [d] Fukui National College of Technology, Fukui, Japan

To cite this Article Mizutani, Tadashi , Yagi, Shigeyuki , Honmaru, Atsushi , Goldacker, Thorsten , Kitagawa, Susumu , Furusyo, Masaru , Takagishi, Toru and Ogoshi, Hisanobu(1999) 'Catalysis of Helix Inversion of Zinc Bilindiones by Amines and Amino Acid Esters', Supramolecular Chemistry, 10: 4, 297 — 308
To link to this Article: DOI: 10.1080/10610279908054513
URL: http://dx.doi.org/10.1080/10610279908054513

SUPRAMOLECULAR CHEMISTRY, Vol. 10, pp. 297–308
Reprints available directly from the publisher
Photocopying permitted by license only

Catalysis of Helix Inversion of Zinc Bilindiones by Amines and Amino Acid Esters

TADASHI MIZUTANI[a,*], SHIGEYUKI YAGI[b], ATSUSHI HONMARU[a], THORSTEN GOLDACKER[a], SUSUMU KITAGAWA[a], MASARU FURUSYO[c], TORU TAKAGISHI[b] and HISANOBU OGOSHI[d]

[a] *Department of Synthetic Chemistry and Biological Chemistry, Graduate School of Engineering, Kyoto University, Sakyo-ku, Kyoto 606-8501, Japan;* [b] *Department of Applied Materials Science, Osaka Prefecture University, Gakuen-cho, Sakai, Osaka 599-8531, Japan;* [c] *CAE Research Center, Sumitomo Electric, Ltd., Hikari-dai 1-7, Seika-cho, Souraku-gun, Kyoto 619-0237, Japan;* [d] *Fukui National College of Technology, Geshi, Sabae, Fukui 916-8507, Japan*

(Received 17 December 1998; In final form 25 February 1999)

Control of the rate of conformational changes of a molecule by intermolecular forces is one of challenging goals in host-guest chemistry. Dynamic ^{1}H NMR studies demonstrated that the conformational change of zinc bilindione complexes was found to be catalyzed by amines. Isomerization of [3,8,12,17-tetraethyl-1,21-dihydro-19-methoxy-2,7,13,18-tetramethyl-23*H*-bilin-1-onato]zinc(II), the zinc chelate of aetiobiliverdin-IV γ, from *P*- to *M*-helical conformation was slow ($k < 1\ s^{-1}$) at 223 K in CD_2Cl_2. It was accelerated up to $k = 13\ s^{-1}$ by adding (*R*)-1-(1-naphthyl)ethylamine (NEA) until all the zinc bilindione was complexed. The rate was further accelerated by the addition of more NEA with smaller dependence on the NEA concentration. The rate of helix inversion was thus catalyzed by one amine molecule, and further accelerated by the second amine molecule. Amino acid esters also showed catalytic activity, although the activity was lower than that of amines. The helix inversion rates were decelerated, as the peripheral alkyl groups introduced at the terminal pyrroles of bilindione became bulkier from methyl, ethyl to propyl groups. Thermal fluctuation, namely, an entropic effect, of these peripheral alkyl groups was responsible for the retardation.

Keywords: Bilindione, conformational change, kinetics, activation entropy

MAIN TEXT

Conformations of biological molecules and natural products are precisely controlled for their proper functions. Thus, a more complete understanding of factors that govern conformational equilibria and dynamics of natural products and their analogs is a current subject of research [1]. For instance, formation of a particular conformer predominantly induced by a signal molecule is one of the general methods to transmit information in biological systems, as seen in allosteric control. To mimic allosteric control, several studies were performed, particularly focusing on the binding-induced conformational changes, using diverse host molecules such as dimeric caffeine [2], biphenyl-crown ethers and crown ether dimers [3], porphyrin aggregates [4], a porphyrin dimer [5], acylproline [6], a glycoluril-bridged naphthalene dimer [7], a synthetic peptide [8], and a pseudocyclophane [9]. It was demonstrated that, in some of these systems,

*Corresponding author. Fax: Int. code +(75) 753-4979, e-mail: mizutani@sbchem.kyoto-u.ac.jp

binding of an effector induced the conformational changes in the host molecule, which then alters the binding affinity of host toward the second guest. These studies clarified the equilibrium nature of the binding-induced conformational changes. As another approach to the allosteric control, binding-induced catalysis in the conformational changes could also be an important strategy to develop the allosteric function. An effector could either catalyze or inhibit the conformational changes, controlling the conformational equilibria kinetically, and giving rise to the desired conformation of host. In this regard, the dynamic aspect of the binding-induced conformational changes is important, yet it has received comparatively little attention so far [10,11].

Most bilindiones adopt a helical conformation [12] and the barrier to interconverting *M* and *P* conformers is relatively low [13]. Owing to the well-defined chiral conformations, their flexibility, and facile detection of conformational equilibria by circular dichroism and ^{1}H NMR spectroscopy, bilindiones are a good model for chiral induction as well as for the kinetic studies of conformational changes. We reported equilibrium aspects of chiral induction in bilindione framework of a zinc complex of bilindione (ZnBD) [14]. In a solution, ZnBD exists as a 1:1 mixture of two enantiomeric helical conformations.

Coordination of chiral guest to the zinc of ZnBD drives the equilibrium between the two enantiomeric helical conformers to a more stable diastereomeric complex. ^{1}H NMR studies indicated that the helix inversion process between two helical conformers was slow on the ^{1}H NMR time scale at low temperature. We report here detailed kinetic studies of conformational changes between enantiomeric helices of ZnBD. We found that (1) amines and amino acid esters catalyzed helix inversion of ZnBD, and (2) bulky alkyl groups introduced at the helix terminal of ZnBD retarded the inversion processes through entropic effects.

RESULTS AND DISCUSSION

Synthesis and Binding Equilibria

To clarify the dynamic behaviors of the zinc bilindione-amine systems, we employed four zinc bilindiones **1**–**4** as hosts and four amines, 1-(1-naphthyl)ethylamine (NEA), 1-cyclohexylethylamine (CHEA), leucine methyl ester (Leu-OMe) and phenylalanine methyl ester (Phe-OMe), as guests. The 19*O*-alkylated zinc bilindiones were used here, since zinc bilindiones bearing a non-protected 19-OH group underwent tautomeric isomerization, which disturbed dynamic NMR studies. Zinc bilindiones **1**–**4** were prepared by a route developed by Lightner [15] and Fuhrhop [16]. In Scheme 1 is shown the synthesis of **2**. Preparation of **1**, **3**, and **4** was reported before [14].

UV/Vis, ^{1}H NMR and CD spectroscopic studies demonstrated that ZnBD formed a complex with various amines and amino acid esters in dichloromethane. The binding behaviors and helical chirality induction were reported in the previous paper [14]. The binding constants for these guests in CH_2Cl_2 at 288 K were 300–660 M^{-1} for amines and 100–120 M^{-1} for amino acid esters. CD spectral studies revealed that all these guests induced *M*-helicity in the bilindione framework. ^{1}H NMR spectra at 223 K showed two sets of well-resolved signals owing to zinc bilindione with *M*-helicity and that with *P*-helicity, from which the enantiomeric excesses at 223 K were determined to be 6–30% for amines and 37–57% for amino acid esters.

Catalysis of Conformational Changes by Amines and Amino Acid Esters

The ^{1}H NMR spectral studies of a solution of **1** and chiral guest in CD_2Cl_2 indicated that (1) the complexation between **1** and the guest was faster on the NMR time scale in the temperature range of 223–288 K, thus the average signals of the complexed and uncomplexed hosts were always

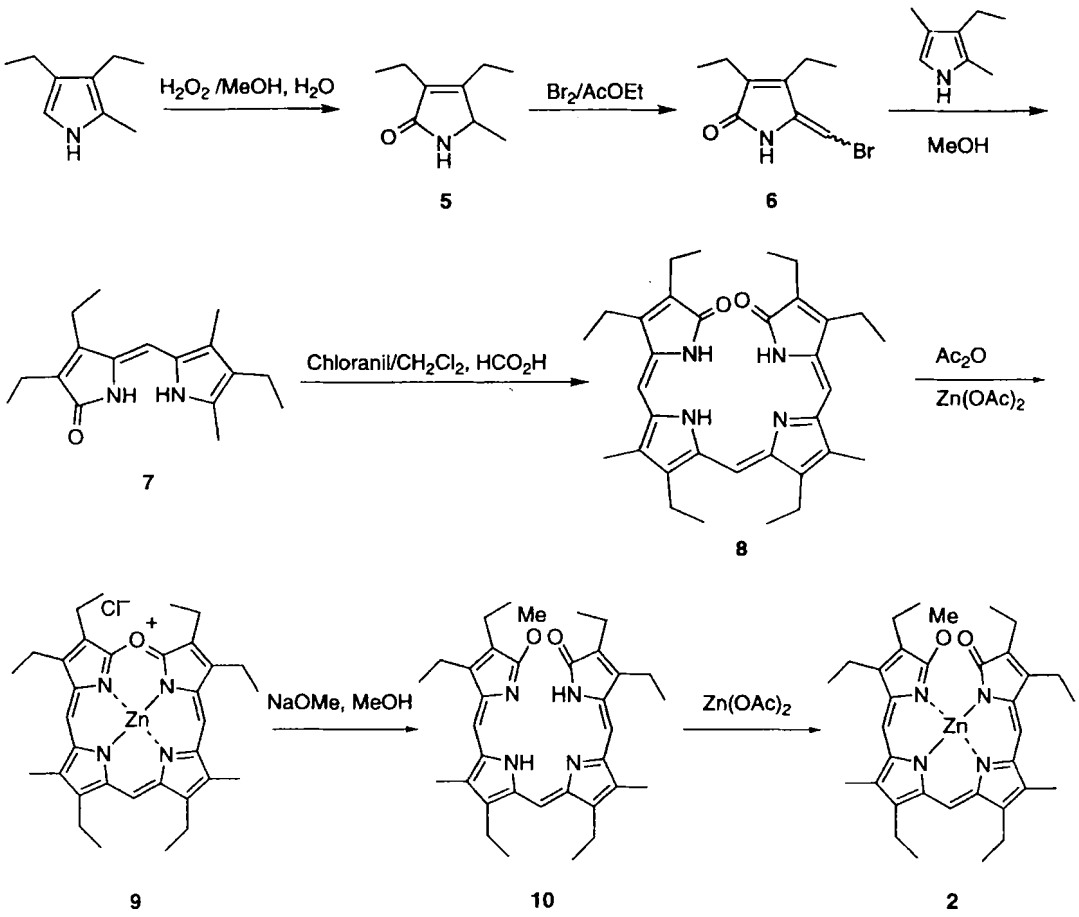

SCHEME 1

observed, and (2) the isomerization between the two enantiomeric forms of **1**, one with *P*-helicity and one with *M*-helicity, was slow on the NMR time scale at low temperatures so that signals were separated by lowering temperature.

The equilibria involved in the system are summarized in Scheme 2 (**L** = amine or amino acid ester). In Scheme 2, (*P*)-**1** and (*P*)-**1**•**L** are indistinguishable by ^{1}H NMR spectroscopy, while (*P*)-**1** + (*P*)-**1**•**L** and (*M*)-**1** + (*M*)-**1**•**L** are distinguishable. As a representative example, variable-temperature ^{1}H NMR spectra of a solution of **1** and an excess amount of (*R*)-NEA in CD_2Cl_2 are shown in Figure 1. The singlet signal for the methoxy protons of **1** of the (*R*)-NEA•(*M*)-**1** complex and that for the (*R*)-NEA•(*P*)-**1** complex appeared as two well-resolved singlets at 4.40 and 4.47 ppm, respectively, at 233 K (Fig. 1(g)). These singlets were coalesced by raising the temperature to 267 K (Fig. 1(c)). We found that the coalescence of the signals also occurred by adding NEA, showing that NEA catalyzed the helix inversion of **1**. To investigate the mechanism of catalysis, the rate constants (k_{obs}) of the isomerization from guest •(*P*)-**1** to guest•(*M*)-**1** in CD_2Cl_2 (Eq. (1)) were determined for varying concentrations of amines by the line shape analysis of the methoxy protons for **1**–**3** and the 10-H and 15-H protons for **4** of the variable-temperature ^{1}H NMR [17].

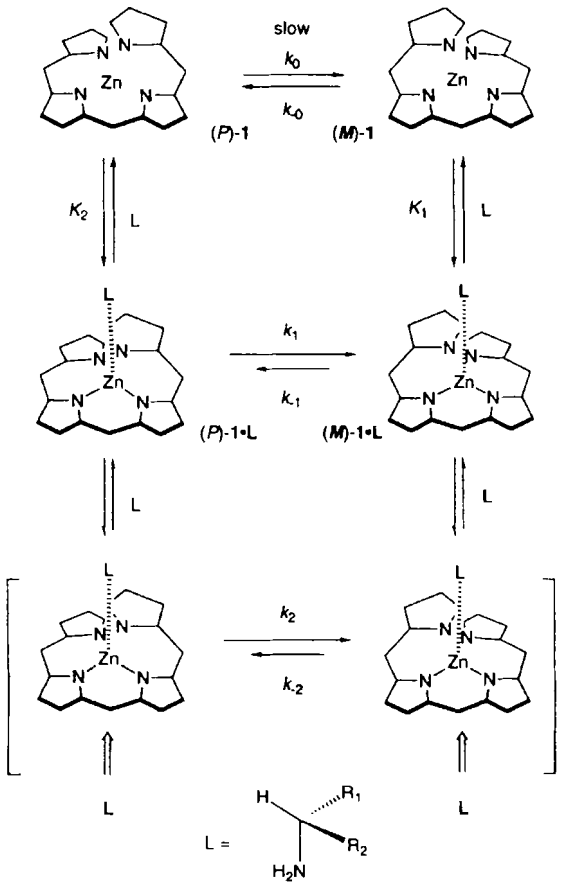

SCHEME 2

$$(P)\text{-}\mathbf{1} + (P)\text{-}\mathbf{1}\bullet(R)\text{-NEA} \underset{k'_{obs}}{\overset{k_{obs}}{\rightleftharpoons}} (M)\text{-}\mathbf{1} + (M)\text{-}\mathbf{1}\bullet(R)\text{-NEA} \quad (1)$$

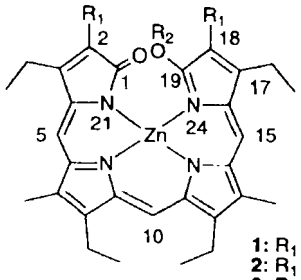

1: $R_1 = CH_3$, $R_2 = CH_3$
2: $R_1 = CH_2CH_3$, $R_2 = CH_3$
3: $R_1 = CH_2CH_2CH_3$, $R_2 = CH_3$
4: $R_1 = CH_3$, $R_2 = CH(CH_3)_2$

Figure 2 shows the plot of k_{obs} at 223 K against the guest concentrations. The rates were accelerated with increasing the guest concentrations. Figure 3 shows the concentration dependence of k_{obs} for NEA at 243 K in more detail. Until all **1** was complexed with NEA ([NEA] < 5 mM), the rate increased rapidly with increasing the NEA concentration. Beyond this concentration ([NEA] = 5 mM), the rate increased linearly with a smaller slope. The rate was too small to determine in this way as the NEA concentration approached zero. These observations indicate that (1) the helix inversion of **1** was slow on the NMR time scale in the absence of NEA [18], (2) the helix inversion was catalyzed by complexation with one molecule of NEA, and (3) the rate was further accelerated by two NEA molecules. Therefore, the helix inversion occurs either *via* the 1 : 1 complex, or *via* the attack of NEA to the

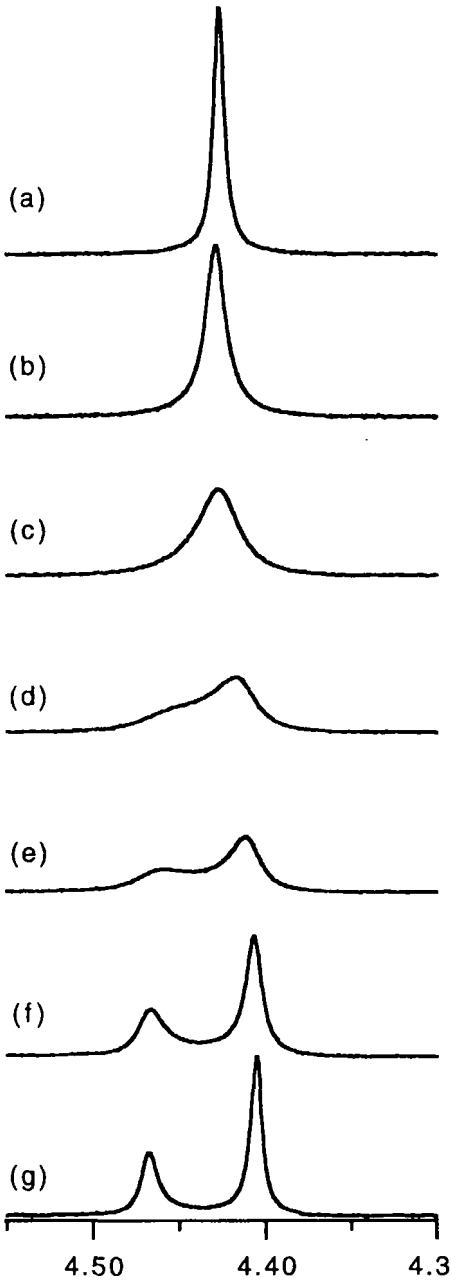

FIGURE 1 Variable-temperature ^{1}H NMR of a solution of **1** and (*R*)-NEA in CD_2Cl_2. $[\mathbf{1}]_0 = 5.07$ mM, $[(R)\text{-NEA}]_0 = 83.5$ mM. (a) 288, (b) 278, (c) 267, (d) 258, (e) 252, (f) 240, and (g) 233 K.

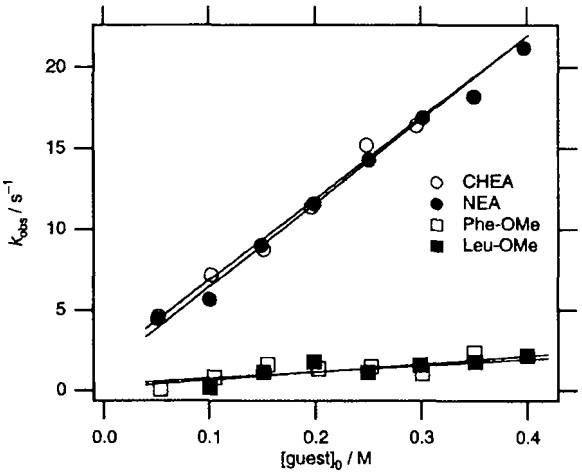

FIGURE 2 Plot of the observed rate constants of the isomerization process from (*P*)-**1** to (*M*)-**1** against the total concentration of (*R*)-CHEA, (*R*)-NEA, L-Phe-OMe, and L-Leu-OMe at 223 K. $[\mathbf{1}]_0 = 4.97 - 5.15$ mM.

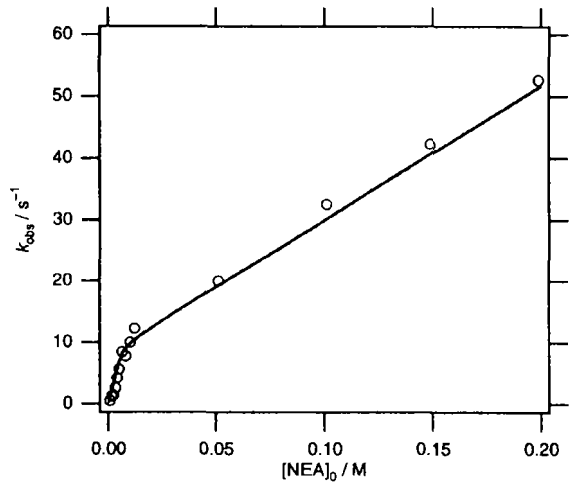

FIGURE 3 Plot of the observed rate constants of the isomerization process from (*P*)-**1** to (*M*)-**1** against the total concentration of (*R*)-NEA, $[(R)\text{-NEA}]_0$, at 243 K. $[(R)\text{-NEA}]_0 = [(R)\text{-NEA}] + [(P)\text{-}\mathbf{1}\bullet(R)\text{-NEA}] + [(M)\text{-}\mathbf{1}\bullet(R)\text{-NEA}]$. $[\mathbf{1}]_0 = 5.02$ mM. The calculated curve based on Eq. (2) is shown.

1 : 1 complex as shown in Scheme 2 [19]. UV/V is and ^{1}H NMR titration experiments indicated that a ZnBD-amine complex with the 1 : 2 molar ratio was not formed under the reaction conditions. Therefore we suppose that the interaction of the second NEA molecule with ZnBD occurs at the transition state. The observed rate constants, k_{obs}, of the conformational change from (*P*)-**1** to (*M*)-**1** in the presence of (*R*)-NEA at 243 K are the sum of three terms, $k_0[(P)\text{-}\mathbf{1}]$, $k_1[(P)\text{-}\mathbf{1}\bullet\text{NEA}]$, and $k_2[(P)\text{-}\mathbf{1}\bullet\text{NEA}][\text{NEA}]$, provided that the ligand exchange is faster than the helix

inversion. Because k_0[(*P*)-**1**] is much smaller than other terms, it is neglected and the observed rate constants were fitted to the following equation:

$$k_{obs} = (k_1[(P)\text{-}\mathbf{1} \bullet \text{NEA}] + k_2[(P)\text{-}\mathbf{1} \bullet \text{NEA}][\text{NEA}])/([(P)\text{-}\mathbf{1}] + [(P)\text{-}\mathbf{1} \bullet \text{NEA}]) \quad (2)$$

where [(*P*)-**1**•NEA] is the concentration of the complex between (*P*)-**1** and (*R*)-NEA [20], k_1 is the rate constant of helix inversion of the 1:1 complex, and k_2 is the rate constant of the helix inversion triggered by the attack of NEA on the 1:1 complex. Curve fitting to the observed rate constants yielded $k_1 = 9.5 \pm 0.7\,s^{-1}$ and $k_2 = 217 \pm 4.6\ M^{-1}s^{-1}$. In the presence of excess amines ($[NEA]_0 \gg [\mathbf{1}]_0$), the concentration of uncomplexed (*P*)-**1** can be neglected compared to the concentration of the (*P*)-**1**•NEA complex. Thus $[(P)\text{-}\mathbf{1}]+[(P)\text{-}\mathbf{1}\bullet\text{NEA}] \approx [(P)\text{-}\mathbf{1}\bullet\text{NEA}]$ and $[NEA] \approx [NEA]_0$, then Eq. (2) can be simplified to Eq. (3).

$$k_{obs} = k_1 + k_2[NEA]_0 \quad (3)$$

The rate constants k_1 and k_2 were determined from the plot of k_{obs} against $[NEA]_0$ by use of Eq. (3).

It was confirmed that the rate constants were not dependent on the concentration of **1**: the values of k_1 of inversion from (*P*)-**1** to (*M*)-**1** in the presence of (*R*)-NEA were 9.5 ($[\mathbf{1}]_0 = 9.9$ mM), 8.5 ($[\mathbf{1}]_0 = 5.0$ mM), and $8.7\,s^{-1}$ ($[\mathbf{1}]_0 = 2.6$ mM), and the values of k_2 were 218 ($[\mathbf{1}]_0 = 9.9$ mM), 228 ($[\mathbf{1}]_0 = 5.0$ mM) and $205\,M^{-1}s^{-1}$ ($[\mathbf{1}]_0 = 2.6$ mM) at 243 K.

Figure 2 shows that amines (NEA and CHEA) had higher catalytic activity than amino acid esters (Leu-OMe and Phe-OMe). The values of k_2 for amines were one order of magnitude larger than those for amino acid esters. The values of $k_2/M^{-1}s^{-1}$ at 223 K are 101 (CHEA), 104 (NEA), 7.7 (Phe-OMe), and 10.0 (Leu-OMe). We suggest that the more basic amines can stabilize the transition state more effectively than amino acid esters.

Transition State of Helix Inversion

The molecular orbital calculations of the transition state of helix inversion at the HF/3-21G level were performed with an ammonia ligand and without any fifth ligand. The transition state structure was optimized by using the synchronous transit-guided quasi-newton (STQN) method. It was confirmed that vibrational analysis gave only one imaginary frequency. For the transition state with one ammonia ligand, the intrinsic reaction coordinate (IRC) analysis was also performed to confirm the reaction path from the transition state structure to the ground state structure. Both transition states are similar in structure: the four nitrogen atoms and zinc are almost in a single plane, while N21 and N24 deviated from the plane in the initial state. Thus, the coordination geometry around the zinc changes from distorted tetrahedral to planar as the transition state is developed (Figs. 4 and 5).

The catalysis by the one and two NEA molecules can be attributable to the stabilization of the transition state through the axial coordination of amines and amino acid esters [21, 22]. The activation energy with ammonia and without ammonia determined by the *ab initio* calculations was 21.4 and 46.0 kcal/mol, respectively. Although the transition state with two ammonia ligands was not obtained yet, these calculations indicated that the transition state of the helix inversion can be stabilized by the

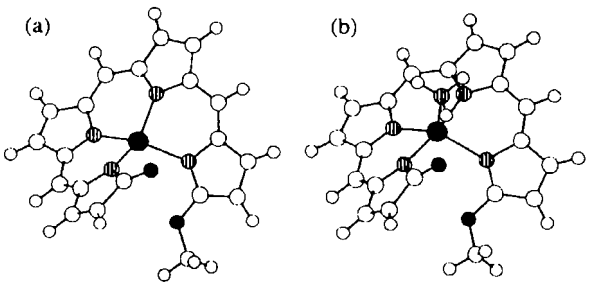

FIGURE 4 The geometry of the ground state of (a) a model compound of **1** and (b) the complex between a model compound of **1** and ammonia. The geometry was optimized at the HF/3-21G level.

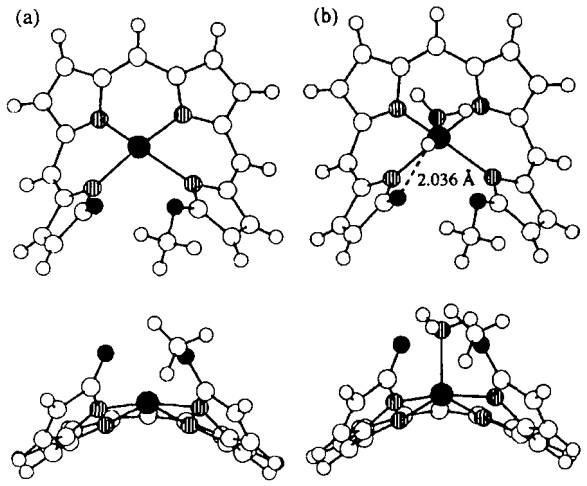

FIGURE 5 The geometry of the transition state (TS) of helix inversion of a model compound of **1** calculated by the MO calculation at the HF/3-21G level. In the model compound, the alkyl groups at the 2, 3, 7, 8, 12, 13, 17, 18-positions of **1** were replaced with hydrogens. (a) The transition state without ammonia. $E = -2895.903234$ (TS), -2895.976602 au (the initial state) (b) The transition state with ammonia. $E = -2951.850251$ (TS), -2951.8844201 au (the initial state).

TABLE I Kinetic parameters for the helix inversion processes from (*R*)-NEA•(*P*)-**1** to (*R*)-NEA•(*M*)-**1** in CD_2Cl_2 determined by Eyring plot[a]

	$\Delta H^{\ddagger}$ (kcal/mol)	$\Delta S^{\ddagger}$ (cal/K/mol)	$\Delta G^{\ddagger}_{253}$ (kcal/mol)	$\Delta G^{\ddagger}_{223}$ (kcal/mol)
1 (Me)	10.7 ± 0.4	-9.4 ± 0.4	13.1	12.8
2 (Et)	9.7 ± 0.7	-15.4 ± 1.5	13.6	13.1
3 (Pr)	9.9 ± 0.3	-15.2 ± 0.6	13.7	13.3

[a]Determined by fitting the data to $\ln (k_1/T) = -\Delta H^{\ddagger}/RT + \Delta S^{\ddagger}/R + \ln (k_B/h)$, where k_B is Boltzmann's constant and h is Planck's constant.

TABLE II Kinetic parameters for the helix inversion processes from (*R*)-NEA•(*P*)-**1** to (*R*)-NEA•(*M*)-**1** catalyzed by (*R*)-NEA in CD_2Cl_2 determined by Eyring plot[a]

	$\Delta H^{\ddagger}$ (kcal/mol)	$\Delta S^{\ddagger}$ (cal/K/mol)	$\Delta G^{\ddagger}_{253}$ (kcal/mol)	$\Delta G^{\ddagger}_{223}$ (kcal/mol)
1 (Me)	6.6 ± 0.4	-20.5 ± 1.5	11.8	11.2
2 (Et)	6.1 ± 0.2	-24.4 ± 0.6	12.2	11.5
3 (Pr)	5.7 ± 0.2	-26.7 ± 0.6	12.4	11.6

[a]Determined by fitting the data to $\ln (k_2/T) = -\Delta H^{\ddagger}/RT + \Delta S^{\ddagger}/R + \ln (k_B/h)$, where k_B is Boltzmann's constant and h is Planck's constant.

coordination of ammonia. The source of the large discrepancy between the observed activation enthalpy (9.7–10.7 kcal/mol) and the calculated activation energy (21.4 kcal/mol) is not clear at this time.

Activation Parameters and Effects of Peripheral Alkyl Groups on Conformational Dynamics

Eyring plot for the inversion rate constants k_1 and k_2 (Eq. 3) for **1**–**3** afforded the activation enthalpy and the activation entropy as listed in Tables I and II.

Both activation enthalpy and activation entropy for k_1 are larger than those for k_2. The larger activation entropy of k_1 than that of k_2 reflects the unimolecular and bimolecular helix inversion processes, respectively. The lower activation enthalpy of k_2 is attributable to the stabilization of the transition state by the amine through electronic interactions.

To examine the effects of the peripheral alkyl groups of ZnBD on the dynamics, we compared the kinetic data of **1** with those of **2** and **3**, in which the alkyl groups at 2- and 18-positions were varied from methyl, ethyl to propyl groups. As the 2- and 18-substituents become bulkier, the rate constant k_2 was reduced by a factor of 3 at 253 K. The kinetic parameters for the k_2 process listed in Table II indicate that (1) an isokinetic relationship [23] with a positive coefficient ($\delta\Delta H^{\ddagger}/\delta\Delta S^{\ddagger}$) [24] holds, and (2) the rate deceleration of **3** compared to **1** and **2** is governed by the negatively larger activation entropy term, although the activation enthalpy is favorable for **3**. Thus the retardation effects of the bulky alkyl groups at 2- and 18-positions on the bimolecular inversion process (k_2) are entropic. Similar trends are seen for the unimolecular inversion process (k_1), although precise determination of the rate constant k_1 was more difficult, and suffered from larger uncertainties.

The helix inversion rate was also affected by the changes in the substituents at the 19*O*-position. 19*O*-Methyl ZnBD (**1**) showed the larger

rate constant k_2 than the 19*O*-isopropyl ZnBD (**4**) as shown in Table III. The ratio of k_2 for **1** to that for **4** ranges from 2.1 to 3.2 in the temperature range of 213–223 K, and increases with increasing temperature. Therefore the retardation effects of the isopropyl group in place of the methyl group is entropic again.

Bartlett *et al.* [25] suggested that, in the decomposition of *t*-butyl peresters, the activation entropy term is related to the number of freedom of bond rotation frozen at the transition state. The negatively larger activation entropy observed in our system indicates that a number of bonds are restricted at the transition state when the substituents at the 2- and 18-positions become bulkier. The geometry of the transition state obtained by the *ab initio* calculations (Fig. 5) indicates that the 1-oxygen and 19-oxygen atoms are in van der Waals contact (the O···O distance was 2.737 Å based on the HF/3-21G calculations). Then the methyl group at the 19-oxygen position is in contact with the alkyl group at the 18-position, which then interacts with the 17-ethyl group. The decrease in entropy of activation with increasing the bulkiness of 2- and 18-alkyl groups would arise from these steric demands for the alkyl groups in the transition state.

It is interesting to compare these results with the thermal racemization of helicenes. The activation parameters of pentahelicene, hexahelicene, and heptahelicene were $\Delta H^{\ddagger} = 22.9$, 35.0, 40.5 kcal/M, respectively, and $\Delta S^{\ddagger} = -4.1$, -4.2, -3.9 cal/K/M, respectively [26]. Therefore, in the thermal recemization of helicenes, the retardation on going from penta-, hexa- to heptahelicene is attributed to the enthalpic effect. The increase in conformational energy can account for this effect.

TABLE III The effects of the alkyl groups on 19-oxygen on the helix inversion rate constants (k_2, $M^{-1}s^{-1}$) from (*P*)-ZnBD to (*M*)-ZnBD in the presence of (*R*)-NEA in CD_2Cl_2

Temperature (K)	k_2(1)	k_2(4)	Ratio, k_2(1)/k_2(4)
223	98	31	3.2
218	58	21	2.8
213	40	19	2.1

The steric repulsion by alkyl groups observed as an entropic effect in this study is in contrast to the enthalpic retardation observed in helicene racemization. Entropic control of conformational dynamics owing to the alkyl groups may be a general strategy to regulate conformational dynamics of molecules with aliphatic substituents including biomolecules.

EXPERIMENTAL SECTION

General

^1H and ^{13}C NMR spectra were recorded at 500 MHz and 125.7 MHz, respectively. ^1H NMR chemical shifts are reported in ppm downfield from internal TMS (0 ppm) in $CDCl_3$ and, relative to residual protons at 5.32 ppm in CD_2Cl_2. ^{13}C NMR chemical shifts are reported in ppm relative to the resonance of $CDCl_3$ at 77.0 ppm. FAB mass spectra were obtained by using 3-nitrobenzyl alcohol as a matrix. The *ab initio* MO calculations were performed by using the Gaussian 94 program package [27]. Full geometry optimization was performed at the Hartree Fock (HF) level using the 3-21G basis set with the Fopt keyword. Optimization of the transition state structure was performed by using the synchronous transit-guided quasi-newton (STQN) method [28] with the qst2 keyword. Frequency calculations and IRC calculations were carried out with freq and irc keywords to confirm the transition state structures.

Materials and Solvents

Amino acid esters for the spectroscopic measurements were prepared by neutralization of their hydrochlorides followed by bulb-to-bulb distillation. L-Phe-OMe•HCl was purchased from Sigma Chemical Company. L-Leu-OMe•HCl was purchased from Nacalai Tesque Chemical Company. (*R*)-NEA was purchased from Tokyo Chemical

Industries and used after distillation. (*R*)-CHEA was purchased from Aldrich Chemical Company, Inc. and used without purification. Preparation of zinc bilindiones **1**, **3**, and **4** was reported previously. Zinc bilindione **2** was similarly prepared as follows.

3,4-Diethyl-2,5-dihydro-5-methyl-2-oxo-1*H*-pyrrole (5)

To a solution of 3,4-diethyl-2-methyl-1*H*-pyrrole [29] (7.92 g, 0.0577 mol) in a mixture of methanol and water (3 : 1, v/v, 65 mL) was added dropwise 30% H_2O_2 (8.74 g, 0.0771 mol) at 55°C. The mixture was stirred for 2 h at the same temperature, and then heated at reflux for 2 h. After cooling, K_2CO_3 (2.99 g, 0.0216 mol) in 20 mL of water was added, followed by stirring overnight at rt. The mixture was neutralized with 1 M HCl, and the methanol in the mixture was removed by evaporation. The residual aqueous solution was extracted with CH_2Cl_2 (60 mL × 3), and the organic layer was washed with water (100 mL × 2) and sat. brine (100 mL), and then dried over anhydrous $MgSO_4$. The solvent was removed, and the residue was purified by distillation at reduced pressure to afford **5** (6.78 g, 0.0442 mol, 77%); bp 143–147°C at 0.6 mmHg, mp 35–40°C; ^{1}H NMR ($CDCl_3$) δ 1.07 (*t*, *J* = 7.6 Hz, 3H), 1.10 (*t*, *J* = 7.6 Hz, 3H), 1.26 (*d*, *J* = 6.7 Hz, 3H), 2.18–2.28 (*m*, 3H), 2.43–2.50 (*m*, 1H), 4.06 (*q*, *J* = 6.7 Hz, 1H), 7.47 (br *s*, 1H); ^{13}C NMR ($CDCl_3$) δ 13.4, 13.6, 16.5, 18.1, 19.3, 53.6, 132.7, 158.8, 174.8; IR (KBr) 3253, 2972, 2935, 2875, 1687, 1462, 1182 cm^{-1}; EI MS (relative intensity) *m*/*z* 153 (98, M^+), 138 (85), 124 (100); HR EI MS calcd for $[C_9H_{15}NO]^+$ 153.1154, found 153.1159; Anal. Calcd for $C_9H_{15}NO \bullet 0.3H_2O$: C, 68.15; H, 9.91; N, 8.83. Found: C, 68.00; H, 10.20; N, 8.59.

5-Bromomethylene-3,4-diethyl-2,5-dihydro-2-oxo-1*H*-pyrrole (6)

To a stirred solution of **5** (6.43 g, 0.0402 mol) in ethyl acetate (60 mL) was added bromine (4.4 mL, 0.085 mol) at 55°C over 1 h. The mixture was heated at reflux with stirring for 15 min. After cooling, the mixture was washed with sat. $NaHCO_3$ (125 mL × 2), water (150 mL) and sat. brine (150 mL), and then dried over anhydrous $MgSO_4$. The solvent was removed by evaporation, and the residue was dispersed with stirring in a mixture of hexane and ethyl acetate (3/1, v/v, 20 mL). The solids were collected by filtration and the filtrate was evaporated to afford an oil, to which a small amount of hexane was added.

The mixture was allowed to stand overnight at −20°C to afford precipitates, which were collected by filtration to yield another solid. All the solids were combined and purified by column chromatography (alumina, CH_2Cl_2 as eluent) to yield **6** as white solids (5.88 g, 0.0255 mol, 61%); mp 99–101°C; ^{1}H NMR ($CDCl_3$) δ 1.12 (*t*, *J* = 7.6 Hz, 3H), 1.16 (*t*, *J* = 7.6 Hz, 3H), 2.32 (*q*, *J* = 7.6 Hz, 2H), 2.42 (*q*, *J* = 7.6 Hz, 2H), 5.91 (*s*, 1H), 7.46 (br *s*, 1H); ^{13}C NMR ($CDCl_3$) δ 13.4, 15.0, 16.9, 17.7, 86.6, 135.1, 141.3, 144.7, 170.9; IR (KBr) 3163, 3041, 2968, 2933, 2973, 1707, 1639, 1207, 725 cm^{-1}; EI MS (relative intensity) *m*/*z* 231 (64, $M^+ + 2$), 229 (66, M^+), 216 (26), 214 (26), 202 (7), 200 (7), 150 (100); HR EI MS calcd for $[C_9H_{12}NO^{79}Br]^+$ 229.0102, found 229.0114; Anal. Calcd for $C_9H_{12}NOBr$: C, 46.98; H, 5.26; N, 6.09. Found: C, 46.94; H, 5.61; N, 6.01.

2,3,8-Triethyl-7,9-dimethyl-1-oxo-1,10-dihydrodipyrrin (7)

A mixture of 3-ethyl-2,4-dimethyl-1*H*-pyrrole (1.50 g, 0.0122 mol) and **6** (2.30 g, 0.0100 mol) in methanol (20 mL) was heated at reflux under an Ar atmosphere for 2 h. After cooling, the mixture was allowed to stand overnight at −20°C to afford yellow precipitates, which were collected by filtration and washed with CH_2Cl_2–MeOH (1:1, v/v, 100 mL). These solids were dried *in vacuo* to afford **6** (1.94 g, 7.12 mmol, 71%) which was used in the next step without further purification; mp 231–235°C (dec); ^{1}H NMR ($CDCl_3$) δ 1.08 (*t*, *J* = 7.6 Hz, 3H), 1.13 (*t*, *J* = 7.6

Hz, 3H), 1.20 ($t, J = 7.6$ Hz, 3H), 2.14 (3H, *s*), 2.38–2.44 (7H, *m*), 2.56 ($q, J = 7.6$ Hz, 2H), 6.15 (*s*, 1H), 10.4 (br *s*, 1H), 11.3 (br *s*, 1H); ^{13}C NMR ($CDCl_3$) δ 9.5, 11.2, 14.3, 15.4, 16.0, 16.9, 17.4, 17.8, 101.3, 122.2, 122.9, 124.5, 126.7, 128.2, 131.1, 147.7, 173.7; IR (KBr) 3359, 3190, 2966, 2926, 2870, 1653, 1633, 1462, 714, 675 cm^{-1}; EI MS (relative intensity) m/z 272 (M^+, 100), 257 (45), 243 (12); HR EI MS calcd for $[C_{17}H_{24}N_2O]^+$ 272.1889, found 272.1884; Anal. Calcd for $C_{17}H_{24}N_2O$: C, 74.96; H, 8.88; N, 10.28. Found: C, 74.57; H, 9.17; N, 10.40.

2,3,8,12,17,18-Hexaethyl-7,13-dimethyl-1,19,21,24-tetrahydro-1,19-bilindione (8)

To a refluxed solution of *p*-chloranil (2.46 g, 10.0 mmol) in CH_2Cl_2 (250 mL) was added dropwise a solution of **7** (1.09 g, 4.00 mmol) in CH_2Cl_2 (300 mL) over an hour, and then formic acid (25 mL) was added at a time. The mixture was heated at reflux for 22 h and condensed to *ca.* 150 mL by distillation, followed by reflux for additional 10 h. The mixture was allowed to stand at −20°C overnight to afford heavy precipitates, which were removed by filtration and washed with small amount of CH_2Cl_2. The filtrate was combined with the washing and neutralized with sat. Na_2CO_3. The organic phase was separated, washed with 1 M NaOH (300 mL × 3), water (500 mL) and sat. brine (500 mL), and dried over anhydrous $MgSO_4$. The solvent was removed by evaporation, and the residue was recrystallized from CH_2Cl_2–MeOH to yield **8** as dark blue crystals (813 mg, 1.54 mmol, 77%); mp 261–265°C (dec); ^{1}H NMR ($CDCl_3$) δ 1.08 ($t, J = 7.6$ Hz, 6H), 1.17 ($t, J = 7.6$ Hz, 6H), 1.23 ($t, J = 7.6$ Hz, 6H), 2.07 (*s*, 6H), 2.28 ($q, J = 7.6$ Hz, 4H), 2.52 ($q, J = 7.6$ Hz, 4H), 2.58 ($q, J = 7.6$ Hz, 4H), 5.91. (*s*, 2H), 6.63 (*s*, 1H) 8.31 (br, 2H); ^{13}C NMR ($CDCl_3$) δ 9.4, 13.6, 15.3, 16.1, 16.9, 17.7, 17.8, 96.3, 113.7, 127.0, 133.7, 139.6, 140.8, 141.5, 146.4, 150.0, 172.1; IR (KBr) 3342, 2964, 2929, 2870, 1695, 1682, 1589, 1215, 1097 cm^{-1}; FAB MS m/z 527 ($M^+ + 1$); HR FAB MS calcd for $[C_{33}H_{42}N_4O_2]^+$ 526.3308, found 526.3288. Anal. Calcd for $C_{33}H_{42}N_4O_2$: C, 75.25; H, 8.04; N, 10.64. Found: C, 74.90; H, 8.24; N, 10.31.

[2,3,7,8,13,17-Hexaethyl-12,18-dimethyl-5-oxoniaporphyrinato]zinc(II) chloride (9)

A mixture of **8** (176 mg, 0.334 mmol), acetic anhydride (6 mL), ethanol saturated with zinc acetate (6 mL) and $ClCH_2CH_2Cl$ (30 mL) was boiled for 30 min in an oil bath with a temperature of 100°C. After cooling, the solvent was removed by evaporation and CH_2Cl_2 (50 mL) was added to the residue. The mixture was washed with 10% NH_4Cl (50 mL × 3), water (50 mL) and sat. brine (50 mL), and then dried over anhydrous $MgSO_4$. The solvent was removed by evaporation and purification of the residue by silica gel column chromatography (20:1 CH_2Cl_2/methanol, v/v, as eluent) followed by recrystallization from CH_2Cl_2-hexane yielded dark blue crystals of **9** (160 mg, 0.263 mmol, 79%). mp > 250°C (dec); ^{1}H NMR ($CDCl_3$) δ 1.61 ($t, J = 7.6$ Hz, 6H), 1.67 ($t, J = 7.6$ Hz, 6H), 1.71 ($t, J = 7.6$ Hz, 6H), 3.05 (*s*, 6H), 3.38–3.59 (*m*, 12H), 9.20 (*s*, 2H), 9.27 (*s*, 1H); ^{13}C NMR ($CDCl_3$) δ 10.7, 15.6, 17.3, 17.5, 18.2, 19.1, 19.2, 112.6, 114.6, 130.6, 135.4, 142.6, 145.9, 147.5, 148.6, 151.8, 163.0; IR (KBr) 2966, 2931, 2872, 1547, 1207, 914 cm^{-1}; FAB MS m/z 571 ($[M-Cl]^+$); HR FAB MS calcd for $[C_{33}H_{39}N_4O^{64}Zn]^+$ 571.2415, found 571.2435.

2,3,8,12,17,18-Hexaethyl-1,21-dihydro-19-methoxy-7,13-dimethyl-22*H*-bilin-1-one (10)

A mixture of **9** (121 mg, 0.199 mmol) and sodium methoxide (32.4 mg, 0.600 mmol) in dry methanol (20 mL) was stirred at rt for 1 h. To the mixture was added $CHCl_3$ (30 mL), followed by washing with 10% NH_4Cl (30 mL). The organic layer was vigorously shaken with phthalate buffer (pH = 4.01, 30 mL × 3), then the dark green solution changed to blue. The organic layer was separated and washed with water (30 mL) and sat. brine (30 mL), dried over anhydrous Na_2SO_4, and then

the solvent was removed by evaporation. Purification of the residue by silica gel column chromatography (75:1 CH_2Cl_2/MeOH, v/v, as eluent) followed by recrystallization from CH_2Cl_2-hexane yielded **10** as dark blue crystals (78.2 mg, 0.145 mmol, 73%); mp 221–224°C (dec); 1H NMR ($CDCl_3$) δ 1.01 ($t, J = 7.6$ Hz, 3H), 1.06 ($t, J = 7.6$ Hz, 3H), 1.13–1.22 (m, 12H), 2.02 (s, 3H), 2.10 (s, 3H), 2.18 ($q, J = 7.6$ Hz, 2H), 2.28 ($q, J = 7.6$ Hz, 2H), 2.44–2.49 (m, 4H), 2.51–2.56 (m, 4H), 4.00 (s, 3H), 5.75 (s, 1H), 6.28 (s, 1H), 6.60 (s, 1H), 10.3 (br s, 1H), 13.0 (br s, 1H); ^{13}C NMR ($CDCl_3$) δ 8.8, 9.6, 13.7, 13.9, 15.5, 16.1, 16.2, 16.3, 16.8, 17.0, 17.5, 17.66, 17.74, 17.9, 55.7, 96.7, 108.0, 115.1, 124.2, 130.8, 130.9, 131.7, 134.8, 135.8, 136.9, 142.9, 144.8, 145.6, 146.7, 148.9, 150.4, 165.5, 171.0, 177.5; IR (KBr) 3327, 2966, 2929, 2868, 1703, 1624, 1589, 1213 cm^{-1}; FAB MS m/z 540 (M^+); HR FAB MS calcd for $[C_{34}H_{44}N_4O_2]^+$ 540.3464, found 540.3452.

Zn(II) complex of 10 (2)

To a solution of **10** (124 mg, 0.229 mmol) in 1 mL of CH_2Cl_2 was added ethanol saturated with zinc acetate (40 mL) and the mixture was heated at reflux for 30 min. After cooling, the solvent was removed by evaporation, and CH_2Cl_2 (50 mL) was added to the residue. The organic solution was washed with water (50 mL × 2) and sat. brine (50 mL), and then dried over anhydrous Na_2SO_4. The solvent was removed by evaporation, and the residue was recrystallized from CH_2Cl_2-hexane to yield **2** as dark green crystals (110 mg, 0.182 mmol, 79%); mp 222–226°C (dec); ^1H NMR (CD_2Cl_2) δ 0.96–1.01 (m, 6H), 1.10–1.15 (m, 9H), 1.19 ($t, J = 7.6$ Hz, 3H), 2.00 (s, 3H), 2.05 (s, 3H), 2.13–2.21 (m, 4H), 2.40 ($q, J = 7.6$ Hz, 2H), 2.46–2.58 (m, 6H), 4.21 (s, 3H), 5.49 (s, 1H), 6.48 (s, 1H), 6.50 (s, 1H); ^{13}C NMR ($CDCl_3$) δ 9.1, 9.2, 13.5, 14.2, 15.8, 16.1, 16.4, 16.5, 16.9, 17.5, 17.9, 18.0, 18.1, 57.2, 93.6, 115.4, 115.8, 127.7, 128.9, 129.5, 136.5, 140.3, 142.2, 145.4, 145.5, 146.6, 146.7, 147.6, 149.0, 156.0, 162.9, 179.7, 181.8; IR (KBr) 2964, 2929, 2868, 1660, 1605, 1574, 1531, 1390, 1273, 1205 cm^{-1}; UV-Vis (CH_2Cl_2, 15°C) $\varepsilon_{403} = 35600$, $\varepsilon_{786} = 17100\ M^{-1}\ cm^{-1}$; FAB MS m/z 602 (M^+); HR FAB MS calcd for $[C_{34}H_{42}N_4O_2{}^{64}Zn]^+$ 602.2600, found 602.2578; Anal. Calcd for $C_{34}H_{42}N_4O_2Zn$: C, 67.60; H, 7.01; N, 9.27. Found: C, 67.30; H, 7.20; N, 9.03.

Acknowledgments

We thank J. Crusats for his valuable discussions on the possible mechanism of helix inversion. We thank T. Kobatake for mass spectroscopic measurements. This work was supported by a Grant-in Aid for Scientific Research from the Ministry of Education, Science, Sports, and Culture, Japan.

References

[1] For a review of design of molecular conformations, see Hoffmann, R. W. (1992). *Angew. Chem.*, **104**, 1147; *Angew. Chem. Int. Ed. Engl.*, **31**, 1124–1134 (1992).
[2] Chen, C.-W. and Whitlock, H. W. Jr. (1978). *J. Am. Chem. Soc.*, **100**, 4921–4922.
[3] (a) Rebek, J. Jr., Trend, J. E., Wattley, R. V. and Chakravorti, S. (1979). *J. Am. Chem. Soc.*, **101**, 4333–4337. (b) Rebek, J. Jr. and Wattley, R. V. (1980). *J. Am. Chem. Soc.*, **102**, 4853–4854. (c) Rebek, J. Jr., Wattley, R. V., Costello, T., Gadwood, R. and Marshall, L. (1980). *J. Am. Chem. Soc.*, **102**, 7398–7400. (d) Rebek, J. Jr., Costello, T., Marshall, L., Wattley, R., Gadwood, R. C. and Onan, K. (1985). *J. Am. Chem. Soc.*, **107**, 7481–7487.
[4] Traylor, T. G., Mitchell, M. J., Ciccone, J. P. and Nelson, S. (1982). *J. Am. Chem. Soc.*, **104**, 4986–4989.
[5] Tabushi, I., Kugimiya, S.-I., Kinnaird, M. G. and Sasaki, T. (1985). *J. Am. Chem. Soc.*, **107**, 4192–4199.
[6] Vincent, C., Hirst, S. C., Garcia-Tellado, F. and Hamilton, A. D. (1991). *J. Am. Chem. Soc.*, **113**, 5466–5467.
[7] Sijbesma, R. P. and Nolte, R. J. M. (1991). *J. Am. Chem. Soc.*, **113**, 6695–6696.
[8] Tabet, M., Labroo, V., Sheppard, P. and Sasaki, T. (1993). *J. Am. Chem. Soc.*, **115**, 3866–3868.
[9] Nabeshima, T., Hashiguchi, A., Yazawa, S., Haruyama, T. and Yano, Y. (1998). *J. Org. Chem.*, **63**, 2788–2789.
[10] (a) Schneider, H.-J. and Werner, F. (1992). *J. Chem. Soc., Chem. Commun.*, pp. 490–491. (b) Hayashi, T., Asai, T., Hokazono, H. and Ogoshi, H. (1993). *J. Am. Chem. Soc.*, **115**, 12210–12211. (c) Kuroda, Y., Lintuluoto, J. and Ogoshi, H. (1994). *Tetrahedron Lett.*, **35**, 3729–3732. (d) Konishi, K., Mori, Y., Aida, T. and Inoue, S. (1995). *Inorg. Chem.*, **34**, 1292–1294. (e) Furusho, Y., Kimura, T., Mizuno, Y. and Aida, T. (1997). *J. Am. Chem. Soc.*, **119**, 5267.
[11] Helix inversion of dinuclear catecholate helicates was reported: Kersting, B., Meyer, M., Powers, R. E. and Raymond, K. N. (1996). *J. Am. Chem. Soc.*, **118**, 7221–7222.

[12] For a review of host-guest chemistry of helical molecules, see Piguet, C., Bernardinelli, G. and Hopfgartner, G. (1997). *Chem. Rev.*, **97**, 2005–2062.

[13] The activation free energy for helix inversion of dimethyl 2-(1-methoxyethyl)-3, 7, 13, 18-tetramethyl-17-vinyl-1, 19-dioxobilin-8,12-dipropionate was determined to be 10 kcal/mol at 205–195 K. See Lehner, H., Riemer, W. and Schaffner, K. (1979). *Liebigs Ann. Chem.*, p. 1798.

[14] Mizutani, T., Yagi, S., Honmaru, A. and Ogoshi, H. (1996). *J. Am. Chem. Soc.*, **118**, 5318–5319. Mizutani, T., Yagi, S., Honmaru, A., Murakami, S., Furusyo, M. Takagishi, T. and Ogoshi, H. (1998). *J. Org. Chem.*, **63**, 8769–8784.

[15] (a) Shrout, D. P. and Lightner, D. A. (1990). *Synthesis*, p. 1062. (b) Shrout, D. P., Puzicha, G. and Lightner, D. A. (1992). *Synthesis*, p. 328.

[16] (a) Fuhrhop, J.-H., Salek, A., Subramanian, J., Mengersen, C. and Besecke, S. (1975). *Liebigs Ann. Chem.*, pp. 1131–1147. (b) Fuhrhop, J.-H., Kruger, P. and Sheldrick, W. S. (1997). *Liebigs Ann. Chem.*, p. 339. (c) Fuhrhop, J.-H. and Kruger, P. (1977). *Liebigs Ann. Chem.*, p. 360.

[17] Rogers, M. T. and Woodbrey, J. C. (1962). *J. Phys. Chem.*, **66**, 540.

[18] As evidence for slow helix inversion in the absence of amines, we observed that the chiral 19*O*-sec-butyl-aetiobiliverdin-IV γ zinc complex showed two sets of signals in CD_2Cl_2 even at 288 K in ^{1}H NMR. For instance, two singlets from the 5-H proton appeared at 5.8 Hz signal separation. Therefore helix inversion is slow on the NMR time scale at 288 K.

[19] Amine catalyzed conformational changes in a porphyrin dimer was reported: Hunter, C. A., Meah, M. N. and Sanders, J. K. M. (1990). *J. Am. Chem. Soc.*, **112**, 5773.

[20] [(*P*) – **1**•NEA] was calculated from the equilibrium constant of the [(*P*) – **1**•(*R*)-NEA] complex, $K_2 = 2890\,M^{-1}$, from the equilibrium constant of the [(*M*) – **1**•(*R*)-NEA] complex, $K_1 = 4570\,M^{-1}$, and the mass balance equations, [(*R*)-NEA]$_0$ = [(*R*)-NEA] + [(*P*) – **1**•(*R*)-NEA]+[(*M*)–**1**•(*R*)-NEA], [**1**]$_0$=[(*P*)–**1**] + [(*M*) – **1**] + [(*P*) – **1**•(*R*)-NEA] + [(*M*) – **1**•(*R*)-NEA], and [(*P*) – **1**] = [(*M*) – **1**].

[21] In the case of biliverdin, the nucleophilic attack of amines at C10 may occur to catalyze the helix inversion, see: Falk, H., Müller, N. and Schlederer, T. (1980). *Monatsh. Chem.*, **111**, 159. With the zinc complex, however, no evidence for the adduct formation was obtained by the ^{1}H NMR, UV-Vis and CD spectra and that mechanism can be excluded.

[22] The equilibrium structure of the complex also supported the conclusion. In the molecular modeling studies of four-coordinated **4** and the five-coordinated **4**-NH_3 complex, using *ab initio* geometry optimization at the HF/3-21G* level, the former adopts more extended conformation (the Cl – C19 distance was 3.68 Å in **4** while it was 3.47 Å in the **4**–NH_3 complex). Therefore the geometry of the latter complex is closer to the transition state than that of the former complex. This can account for the stabilization due to the fifth ligand.

[23] Leffler, J. E. and Grunwald, E., *Rates and Equilibria of Organic Reactions*; John Wiley and Sons, Inc.: New York, 1963, Chapter 9.

[24] The slope of the plot of $\Delta H^{\ddagger}$ against $\Delta S^{\ddagger}$ is 153 K although only three data points are available.

[25] Bartlett, P. D. and Hiatt, R. R. (1957). *J. Am. Chem. Soc.*, **80**, 1398–1405.

[26] The kinetic parameters for the racemization of helicenes are reported. (a) Wynberg, H. and Groen, M. B. (1969). *J. Chem. Soc., Chem. Commun.*, pp. 964–965. (b) Martin, R. H. and Marchant, M. J. (1974). *Tetrahedron*, **30**, 347–349. (c) Borkent, J. H. and Laarhoven, W. H. (1978). *Tetrahedron*, **34**, 2565–2567. (d) Yamada, K.-I., Nakagawa, H. and Kawazura, H. (1986). *Bull. Chem. Soc. Jpn.*, **59**, 2429–2432.

[27] Frisch, M. J., Trucks, G. W., Schlegel, H. B., Gill, P. M. W., Johnson, B. G., Robb, M. A., Cheeseman, J. R., Keith, T., Petersson, G. A., Montgomery, J. A., Raghavachari, K., Al-Laham, M. A., Zakrzewski, V. G., Ortiz, J. V., Foresman, J. B., Cioslowski, J., Stefanov, B. B., Nanayakkara, A., Challacombe, M., Peng, C. Y., Ayala, P. Y., Chen, W., Wong, M. W., Andres, J. L., Replogle, E. S., Gomperts, R., Martin, R. L., Fox, D. J., Binkley, J. S., Defrees, D. J., Baker, J., Stewart, J. P., Head-Gordon, M., Gonzalez, C. and Pople, J. A. *Gaussian 94, Revision E.2*, Gaussian, Inc., Pittsburgh, PA, 1995.

[28] Peng, C. and Schlegel, H. B. (1989). *J. Chem. Phys.*, **90**, 2154.

[29] Dolphin, D., Harris, R. L. N., Huppatz, J. L., Johnson, A. W. and Kay, I. T. (1966). *J. Chem. Soc.* (C), pp. 30–40.